ANALYTIC-NUMERIC METHODS IN THE VALIDATION OF ANY FLOW REGIMES IN HYDRO-AERODYNAMICS

Mircea LUPU[*], Gheorghe RADU[**], Cristian-George CONSTANTINESCU[**]

[*]"Transilvania" University, Faculty of Mathematics and Computer Science, Braşov, Romania (m.lupu@unitbv.ro)
Member of The Academy of Romanian Scientists
[**]"Henri Coandă" Air Force Academy, Braşov, Romania (gh.radu@gmail.com, c.g.constantinescu@gmail.com)

DOI: 10.19062/2247-3173.2017.19.1.46

Abstract: *In this paper there are studied two kinds of problems about a fluid flow or a hot transfer regime. The first problem refers to a parabolic type of a laminar or viscous fluid flow or a hot transfer in a plane or cylindrical domain. It is considered an inverse problem: knowing the data on the boundary of the domain, a method to find the viscosity coefficient or the hot transfer coefficient is given. The best numerical results may be obtained when the number of measurements is increased. The second problem refers to the free boundary flow in the presence of a curvilinear symmetrical obstacle. There are considered the Helmholtz problem when the fluid is unlimited and the Rethi-Jacob scheme when a jet of fluid is forked by a symmetrical obstacle. The problems where studied using singular integral equations and the shapes of the maximal drag obstacle are obtained.*

Keywords: *parabolic equations, the trapeze formula, viscosity coefficient, inviscid jets, nonlinear operator, optimal design.*

1. DETERMINING THE COEFFICIENT FROM THE PARABOLIC TYPE EQUATION

The mathematical modeling of viscous fluid flows, the heating and cooling problems, metal melting, ice melting, wood drying, dispersion or aggregated, mass and heat transfer lead to partial derivate equations of a parabolic type. The viscosity coefficients appear in these equations, humidity coefficients or dispersion – they can be both constant and variable. We present a method to determinate these coefficients when they are not stationary, in the plane case or cylindrical, having input data regarding the speed or the tension on the boundary, or the temperature and the thermal flow changed with the exterior, [8] [3].

A. We consider the parabolic equation:

$$k(t)\frac{\partial w}{\partial t}=\frac{\partial^2 w}{\partial x^2}+F(x,t), w=w(x,t), x\in[0,l], t\geq 0 \tag{1}$$

Representing the plane flow between two plates or the thermal process delimited by the *x=0, x=h* plates. For start we will consider the homogeneity case *E(x,t)=0* and assume that we have the following information *w(x,t)*:

$$w(x,t=0)=f(x) \quad (2)$$
$$w(x=0,t)=g(t),w(x=l,t)=h(t) \quad (3)$$
$$\left.\frac{\partial w}{\partial x}\right|_{x=0}=G(t),\left.\frac{\partial w}{\partial x}\right|_{x=l}=H(t) \quad (4)$$

The conditions (2)-(4) are actually Sturm-Liouville type conditions and have physical meanings related to the according studied problems: so, viscous fluids the conditions (3) of Couette type [3] show the mobility of the plates with speeds *g(t),h(t)* and the relation (4) shows the tensions that emerge between the fluid and the plates. For the caloric problem, *w* is the temperature, (3) the walls heating, (4) the caloric flow between the inside and the outside trough the walls.

Having these data we will present methods to find the coefficient *k(t)* with the conditions (2)-(4) or by weakening them. In order to perform calculations in these continuous environments we impose the non polarity conditions for data, meaning:

$$g(0)=f(0),h(0)=f(l),G(0)=f^{'}(0),H(0)=f^{'}(l) \quad (5)$$

along with the continuity of the simple and partial derivates.

We integrate the equation (1) with respect to *x*

$$k(t)\int_0^l \frac{\partial w}{\partial t}dx=\int_0^l \frac{\partial}{\partial x}\left(\frac{\partial w}{\partial x}\right)dx=\left.\frac{\partial w}{\partial x}\right|_{x=l}-\left.\frac{\partial w}{\partial x}\right|_{x=0}=H(t)-G(t) \quad (6)$$

We apply in the integral the trapeze formula and together with (3) we have:

$$k(t)\frac{l}{2}\left[\left(\frac{\partial w}{\partial t}\right)_{x=l}+\left(\frac{\partial w}{\partial t}\right)_{x=0}\right]=k(t)\frac{l}{2}\left[h^{'}(t)+g^{'}(t)\right]\approx H(t)-G(t) \quad (7)$$
$$k(t)\approx\frac{2\left[H(t)-G(t)\right]}{l\left[h^{'}(t)+g^{'}(t)\right]} \quad (8)$$

If in (1) appears also *F(x,t)* then besides H-G we add U= $\int_0^l F(x,t)dx$. We notice that *k(t)* is retrieved and we have not use (2) ***f(x)*** – although, this will definitely be used if *w(x,t)* is numerically determined in (8) we notice the validity condition $H \neq G$ meaning the plates are not moving parallel with *Ox* simultaneous with constant speed. The formula (8) will be correct as much as in order to apply the trapeze formula we will consider on [0,*l*] multiple nodes having $x_i=i\frac{l}{n},i=0,1,\dots,n$ with $w(x,t)=h(x_i,t),h^{'}(x_i,t)=\frac{\partial w(x_i,t)}{\partial t}$.
In the end results, with these data, applying the trapeze formula,

$$k(t)\approx\frac{H(t)-G(t)}{\frac{l}{n}\left[\frac{h^{'}(t)+g^{'}(t)}{2}+\sum_{i=1}^{n-1}h_t^{'}(x_i,t)\right]} \quad (9)$$

Lets' obtain *k(t)* if one information, either *H(t)* or *G(t)* is missing – the case when *G(t)* is missing from (3), (4); we apply the same operations:

$$h(t)-g(t)=w(l,t)-w(0,t)=\int_0^l \frac{\partial w}{\partial x}(s,t)ds \tag{10}$$

$$\int_\xi^l \frac{\partial^2 w}{\partial x^2}dx=\int_\xi^l W(s,t)ds=\frac{\partial w}{\partial x}(l,t)-\frac{\partial w}{\partial x}(\xi,t) \tag{11}$$

$$\frac{\partial w}{\partial x}(\xi,t)=H(t)-\int_\xi^l W(s,t)ds, \frac{\partial^2 w}{\partial x^2}=W(x,t)=k(t)\frac{\partial w}{\partial t} \tag{12}$$

We replace (12) in (10) and we will apply the Dirichlet formula for the iterate integral

$$\int_a^b d\xi\int_a^\xi W(s,t)ds=\int_a^b ds\int_\xi^b W(s,t)d\xi=\int_a^b (b-\xi)W(s,t)ds$$

$$h(t)-g(t)=lH(t)-\int_0^l (l-s)W(s,t)ds\approx lH(t)-\frac{l^2}{2}W(0,t) \tag{13}$$

$$h(t)-g(t)\approx lH(t)-k(t)\frac{l^2}{2}\frac{\partial w}{\partial t}\bigg|_{x=0}=lH(t)-k(t)\frac{l^2 g^{'}(t)}{2} \tag{14}$$

$$k(t)\approx\frac{2[lH(t)-h(t)+g(t)]}{l^2 g^{'}(t)}=k_H(t) \tag{15}$$

In (13) we applied the trapeze formula, formulas (2) and (3), obtaining (15) comparable with (8); the trapeze formula can be applied on more nodes obtaining a formula comparable with (9). If *G(t)* is present and *H(t)* missing the reasoning in identical obtaining:

$$k(t)\approx\frac{2[h(t)-g(t)-lG(t)]}{l^2 g^{'}(t)}=k_G(t) \tag{16}$$

It can be noticed that the formulas (8) (15) (16) are not identical; for a greater precision we must use the (9) type formulas; because of the data structure and presentation we can build an optimal control problem to exactly determine *k(t)* [1]: Determine the *k* control that minimizes the functional *I(k)*

$$I(k)=\int_0^T\left[\left(\frac{\partial w}{\partial x}(0,t)-G(t)\right)^2+\left(\frac{\partial w}{\partial x}(l,t)-H(t)\right)^2\right]dt\to\min \tag{17}$$

With the restrictions (1) (2) (3) if minimum is zero then w is the solution satisfying (1) (2) (3).

B. The case of cylindrical coordinates (coaxial cylinders with radius $r_1 \lhd r_2$) or the circular crown domain; it is studied considering the equation and conditions [3] [8] for Couette type movements or with gravity and pressure difference trough *F(r,t)*

$$k(t)\frac{\partial w}{\partial t}=\frac{1}{r}\frac{\partial}{\partial r}\left(r\frac{\partial w}{\partial r}\right)+F(r,t), w=w(r,t), r_1 \lhd r \lhd r_2 \tag{18}$$

$$w(r,t=0)=f(r) \tag{19}$$

$$w(r_l,t)=g_1(t), w(r_2,t)=g_2(t) \tag{20}$$

$$\left.\frac{\partial w}{\partial r}\right|_{r=r_1}=G_1(t), \left.\frac{\partial w}{\partial r}\right|_{r=r_2}=G_2(t) \tag{21}$$

Using the same rationale we get *k(t)*: we apply the trapeze formula after we integrate with respect to *r* (18).

$$\mathrm{r}k(t)\frac{\partial w}{\partial t}=\frac{\partial}{\partial r}\left(r\frac{\partial w}{\partial r}\right); k(t)\int_{r_1}^{r_2}\rho\frac{\partial w}{\partial t}(\rho,t)d\rho=r_2G_2-r_1G_1 \tag{22}$$

$$k(t)\frac{r_2-r_1}{2}\left[r_1\frac{\partial w}{\partial t}(r_1,t)+r_2\frac{\partial w}{\partial t}(r_2,t)\right]\approx r_2G_2(t)-r_1G_1(t) \quad \text{meaning}$$

$$k(t)\approx\frac{2}{r_2-r_1}\frac{r_2G_2(t)-r_1G_1(t)}{r_1g_1^{'}(t)+r_2g_2^{'}(t)} \tag{23}$$

For a greater precision we split the interval $[r_1,r_2]$ in *n* parts with $r_i=i\frac{r_2-r_1}{n}$ and the integral from (22) we apply the trapeze formula, obtaining a type (9) formula

$$k(t)\approx\frac{2n}{r_2-r_1}\frac{r_2G_2(t)-r_1G_1(t)}{r_1g_1^{'}(t)+r_2g_2^{'}(t)+2\sum_{i=1}^{n-1}r_ig_i^{'}(t)} \tag{23$'$}$$

If in (18) appears *F(r,t)* then in formulas $(23)(23^{'})(25)$ *U* is added the upper side of the fraction $r_2G_2-r_1G_1+U(r,t)$ where $U(r,t)=\int_{r_1}^{r_2}rF(r,t)dr$ and $G_2(t)=\frac{1}{R}\int_0^R rF(r,t)dr$. It can be noticed that in $(23)(23^{'})$ we have the validity condition for the experimental case so that $r_2G_2(t)\neq r_1G_1(t)$.

If we have the circular cylinder of radius *R*, $r_1=0, r_2=R$ and $G_1(t)$ is missing, we integrate (18) and apply the trapeze formula on the interval [0,*R*] obtaining *k(t* :

$$k(t)\int_0^R r\frac{\partial w}{\partial t}(r,t)dr=r\left.\frac{\partial w}{\partial t}\right|_{r=0}^{r=R}=RG_2(t)$$

$$k(t)\approx\frac{2}{R}\frac{G_2(t)}{g_1(t)} \tag{24}$$

Since the approximation is wide, we split [0,*R*] in n parts with $r_i=i\frac{R}{n}$ obtaining with data $w(r_i,t)=g_i(t)$

$$k(t) \approx \frac{G_2(t)}{\frac{R}{2n}\left[2\sum_{i=1}^{n-1} r_i g_i^{'}(t) + R g_R^{'}(t)\right]} \quad (25)$$

In an analog manner we can formulate the optimal control problem for the determination of *k(t)* : Determine the control *k(t)* which minimize the functional *I[k]* [1]:

$$I(k) = \int_0^T \left[\left(\frac{\partial w}{\partial r}(r_1,t) - G_1(t) \right)^2 + \left(\frac{\partial w}{\partial r}(r_2,t) - G_2(t) \right)^2 \right] dt \to \min$$

with the restriction (18) (19) (20). The method can be applied numerical and experimental in biology, thermal processes, drying, melting, diffusion etc. with practical data observable on measure machines, determining this way the coefficient *k(t).*

2. THE STUDY OF POTENTIAL PLANE FLOWS WITH STREAM LINES FOR INCOMPRESSIBLE FLUIDS IN THE PRERSENCE OF SYMMETRICAL CURVILINEAR PROFILES

We consider the potential plane flows, with free lines, for incompressible fluids in the presence of symmetrical profiles in two cases: first case – curvilinear obstacle in free unlimited stream (based on Helmholtz schema) [9] and the second case – fluid streams, upstream delimited by the height *h*, forked by a symmetrical obstacle, the stream lines at infinity having the asymptotic angle γ (the Rethi-Jacob model) [2].

The obstacles have the same length *L* and in each situation we'll have three sub-cases: 1st case – curvilinear obstacle convex toward downstream, 2nd case – straight perpendicular plate and 3rd case – curvilinear obstacle convex toward upstream (fig. I1, I2, I3) [6] and for the second situation we have the same obstacles in the presence of the limit stream with γ, asymptotic angle (fig. II1, II2, II3).

The studies we made [4], [5] considered the as helping canonical domain – the half plane $\varsigma = \xi + i\eta, \eta \geq 0$ and the Jukovski function $\omega(\varsigma) = t + i\theta = \ln\frac{V^0}{V} + i\theta, V < V^0$ where V^0 is the fluid speed on the free lines, *V* is the speed modulus $|w| = V, \overline{w} = u - iv = \frac{df}{dz}$, $\theta = \arg w$, $\overline{w} = V^0 e^{-\infty}$. We'll consider the physical domain D_z, D_f the potential domain, D_ω the hodographic domain and D_ς the canonical domain, where:

$$f(z) = \varphi(x,y) + i\psi(x,y), \qquad \overline{w} = \frac{df}{dz} = Ve^{-i\theta} \quad (26)$$

the complex potential were determined *f* = *f(*ς*)* for the two situations $f_I(\varsigma) = A\varsigma,\ f_{II}(\varsigma) = \frac{q}{2\pi}\ln(\varsigma - a) + \frac{iq}{2}$ where *A*, *a* are the parameters a>1 and q is the stream debit of width *h*. We determine $\omega = \omega(\varsigma)$ and so $W = W(\varsigma)$; in this manner, from

$\frac{df}{dz} = \frac{df}{d\varsigma}\frac{d\varsigma}{dz}$ we get $z = z(\varsigma)$ and the correspondent D_z, D_f, D_ω, D_w with D_ς conformal transformations, and trough transitivity *f=f(z), w=w(z)* .

$$\omega(\varsigma) = \frac{\sqrt{1-\varsigma}}{\pi}\int_{-1}^{1}\frac{\theta(s)}{\sqrt{1-s}}\frac{ds}{s-\varsigma}\ , \qquad \omega(\varsigma) = \frac{\sqrt{\varsigma+1}}{i\pi}\int_{-1}^{1}\frac{t(s)}{\sqrt{s+1}}\frac{ds}{s-\varsigma}$$

The singular integral equations resulted from determining $\omega(\varsigma)$ which links dual $\theta(\xi)$ with $t(\xi)$, $\xi \in (-1,1)$ are, for the two situations the followings [4] [5] [6] (obtained with Sohotski – Plemelj formula)

$$t(\xi) = \frac{\sqrt{1-\xi}}{\pi}\int_{-1}^{1}\frac{\theta(s)}{\sqrt{1-s}}\frac{ds}{s-\xi}, \qquad \theta(\xi) = -\frac{\sqrt{\xi+1}}{\pi}\int_{-1}^{1}\frac{t(s)}{\sqrt{s+1}}\frac{ds}{s-\xi} \qquad (27)$$

For the 1st situation the upstream asymptotic angle is $\gamma \equiv 0$ and for the 2nd situation:

$$\gamma(a) = \frac{\sqrt{a+1}}{\pi}\int_{-1}^{1}\frac{t(s)}{\sqrt{s+1}}\frac{ds}{a-s}; \qquad k = \frac{L}{h} = \frac{1}{\pi}\int_{-1}^{1}\frac{V^0}{V(\xi)}\frac{d\xi}{a-\xi} = \frac{1}{\pi}\int_{-1}^{1}\frac{e^{t(\xi)}d\xi}{a-\xi} \qquad (28)$$

where *k* is the connection report from which we find the values for a parameter, knowing *k* and the speed distribution on the profile $V = V(\xi)$ or $t = t(\xi), \xi \in (-1,1)$.
The formulas (27) allow solving reverse problems, with $t(\xi)$ or $\theta(\xi)$ given on the profile, the profile shape is determined, for cases (26), (28), $V = V(\xi)$ will be given and $\theta(\xi)$ determined, and for (27) of the plate $\theta = \pi/2$ is determined $V = V(\xi), t = t(\xi)$.
The aero dynamical and geometric parameters for the presented 6 cases are represented in the tables below [4] [5] [6].

Cases I1, I2, I3 based on Helmholtz schema [6]:

Curvilinear Profile

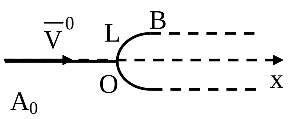

Fig. I1

Helmholtz Schema

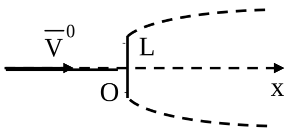

Fig. I2

The impermeable parachute

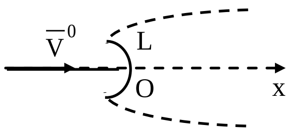

Fig. I3

Parameters in $f = f(\zeta)$ will be:

$$f(\varsigma) = A\varsigma, A = \frac{LV^0}{4} \qquad f(\varsigma) = A\varsigma, A = \frac{2LV^0}{\pi+4} \qquad f(\varsigma) = A\varsigma, A = \frac{LV^0}{4e}$$

The speed distribution on the profile:

$$V_1 = V^0\sqrt{\frac{1+\xi}{2}}\,; \qquad V_2 = V^0\left(\frac{\sqrt{2}-\sqrt{1-\xi}}{\sqrt{2}+\sqrt{1-\xi}}\right)^{1/2} \approx \frac{V_0}{2}\sqrt{\frac{1+\xi}{2}}\,; \qquad V_3 = \frac{V^0}{e}\sqrt{\frac{1+\xi}{2}}\,.$$

The curvilinear obstacle's tangent angle:

$$\theta_1 = \frac{\pi}{2} - T\left[\sqrt{\frac{1+\xi}{2}}\right] < \frac{\pi}{2}\,; \qquad \theta_2 = \frac{\pi}{2}\,; \qquad \theta_3 = \frac{\pi}{2} + \frac{1}{\pi}\ln\frac{\sqrt{2}+\sqrt{1+\xi}}{\sqrt{2}-\sqrt{1-\xi}} - T\left[\sqrt{\frac{1+\xi}{2}}\right] > \frac{\pi}{2}\,.$$

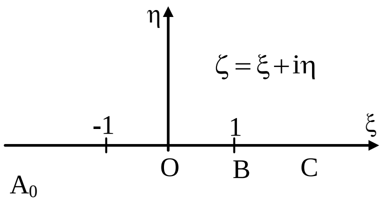

Pressures resultant:

$$P_1 = \frac{\rho V^{0^2} L}{\pi}\,; \quad P_2 = \frac{\rho V_0^2 L}{2}\frac{2\pi}{\pi+4}\,; \quad P_3 = \frac{\rho V^{0^2} L}{2} J[t] \quad \text{with} \quad J[t] = \frac{\left(\int_{-1}^{1}\frac{t(s)}{\sqrt{1+s}}ds\right)^2}{\int_{-1}^{1} e^{t(s)}ds}\,.$$

The distribution V_3 was obtained by extending J[t] with the Jensen inequality for $t_3 = 1 + \ln\sqrt{\frac{2}{1+\xi}}$ [5].

The resistance coefficient:

$$C_x^1 = \frac{2}{\pi} \cong 0{,}637\,; \qquad C_x^2 = \frac{2\pi}{\pi+4} \cong 0{,}87980\,; \qquad C_x^3 = \frac{8}{\pi e} \cong 0{,}936797\,;$$

$$C_x = \frac{2P}{\rho V^0 L}, C_x^1 < C_x^2 < C_x^3(\max imal)\,.$$

Cases II1, II2, II3 limited stream of width h, forked by obstacle:

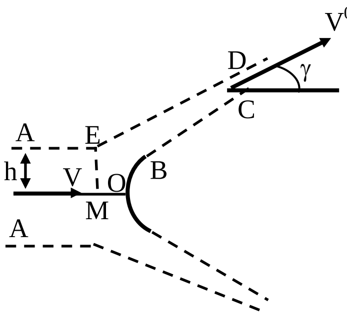

Fig. II1

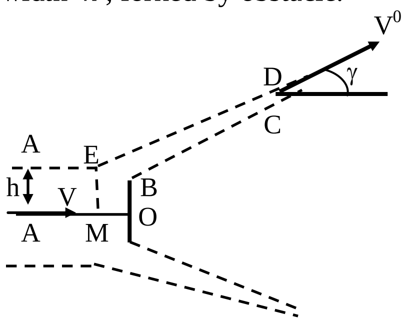

Fig. II2

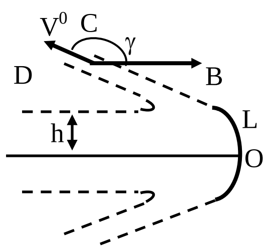

Fig. II3

$$V_1 = V^0\sqrt{\frac{1+\xi}{2}}\,; \quad V_2 = V^0\left(\frac{\sqrt{2}-\sqrt{1-\xi}}{\sqrt{2}+\sqrt{1-\xi}}\right)^{1/2} \approx \frac{V_0}{2}\sqrt{\frac{1+\xi}{2}}\,; \quad V_3 = \frac{V^0}{e}\sqrt{\frac{1+\xi}{2}}\,; \quad V_1 < V_2 < V_3\,.$$

The value of angle θ on the profile:

$$\theta_{1h} = \frac{\pi}{2} - T\left[\sqrt{\frac{1+\xi}{2}}\right] < \frac{\pi}{2}; \quad \theta_{2h} = \frac{\pi}{2}; \quad \theta_{3h} = \frac{\pi}{2} + \frac{1}{\pi}\ln\frac{\sqrt{2}+\sqrt{1+\xi}}{\sqrt{2}-\sqrt{1-\xi}} - T\left[\sqrt{\frac{1+\xi}{2}}\right] > \frac{\pi}{2};$$

$$T[u] = \frac{1}{\pi}\int_0^{\upsilon} \ln\frac{1+u}{1-u}\frac{du}{u}, \quad u \in [0,1], \frac{\partial T}{\partial u} > 0.$$

The asymptotic angle $\gamma(h)$ downstream:

$$\gamma_{1h}(a) = T\left[\sqrt{\frac{2}{a+1}}\right]; \; \gamma_{2h}(a) = arctg\sqrt{\frac{2}{a-1}} \; ; \; \gamma_{3h}(a) = T\left[\sqrt{\frac{2}{a+1}}\right] + \frac{1}{2}\ln\frac{\sqrt{a+1}+\sqrt{2}}{\sqrt{a+1}-\sqrt{2}}.$$

$\gamma_h(a)$ is descendant with respect to *h* and ascendant for $\theta(\xi)$ [6] [7].

$$\gamma_{1h} < \gamma_{2h} < \gamma_{3h} = \gamma_{\max}; \quad 0 < \gamma_1 < \frac{\pi}{4}; \quad 0 < \gamma_2 < \frac{\pi}{2}; \quad 0 < \gamma_3 < \pi.$$

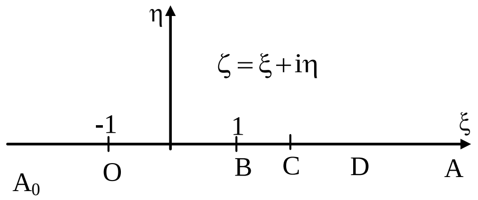

With $\lim\limits_{h\to\infty, a\to\infty} \gamma(h(a)) = 0$ we get case I from II.

If the reports $k = \frac{L}{h}$ are given is found and then a^*:

$$k_1^{(u)} = \frac{1}{\pi}u\ln\frac{u+1}{u-1}; \qquad k_2^{(u)} = 1-\sqrt{1-u^2} + \frac{1}{\pi}u\ln\frac{u+1}{u-1}; \qquad k_3^{(u)} = \frac{e}{\pi}u\ln\frac{u+1}{u-1}.$$

$k = \frac{L}{h} \Rightarrow k_1 < k_2 < k_3$ with $u^* = \sqrt{\frac{2}{a+1}} < 1$. Given $k \Rightarrow u = u^* \Rightarrow a = a^*$.

$$C_x^1(h) = \frac{2[1-\cos\gamma_1(h(a^*))]}{k_1}; \; C_x^2(h) = \frac{2[1-\cos\gamma_2(h(a^*))]}{k_2}; \; C_x^3(h) = \frac{2[1-\cos\gamma_3(h(a^*))]}{k_3};$$

$$C_x^1(h) < C_x^2(h) < C_x^3(h).$$

For k and L fixed we get: $\gamma_1(h) < \gamma_2(h) < \gamma_3(h)$. We can notice that $C_x(h)$ is ascendant with respect to $\gamma(h), \frac{\partial C_x(h)}{\partial \gamma(h)} > 0$, meaning $C_x(h)$ is ascendant in h and, if $h \to \infty, \frac{\partial C_x(h)}{\partial \gamma(h)} > 0$ then $\lim\limits_{h\to\infty} C_x(h) = C_x$.

$$C_x^1(h) \xrightarrow{h\to\infty} C_x^1 = \frac{2}{\pi}; \qquad C_x^2(h) \xrightarrow{h\to\infty} \frac{2\pi}{\pi+4}; \qquad C_x^3(h) \xrightarrow{h\to\infty} \frac{8}{\pi e}.$$

As a result we obtain a way to go from 2nd case, trough flow's width enlargement $u \to \infty, h \to \infty$, to the 1st situation – obstacle in unlimited fluid (Helmholtz version) [7] [6].

We represent $C_x(h)$ with the help of the asymptotic angle γ: $\gamma = \gamma(u) \Rightarrow u = f^{-1}(\gamma)$.

$$\gamma_1(h) = T(u) = f_1(u); \quad \gamma_2(h) = arctg\frac{u}{\sqrt{1-u}} = f_2(u); \quad \gamma_3(h) = T(u) + \frac{1}{2}\ln\frac{1+u}{1-u} = f_3(u);$$

$$u = f_1^{-1}(\gamma_1); \qquad u = f_2^{-1}(\gamma_2) \qquad u = f_3^{-1}(\gamma_3)$$

$$C_x^1(h) = \frac{2[1-\cos f_1(u)]}{k_1(u)}; \qquad C_x^2(h) = \frac{2[1-\cos f_2(u)]}{k_2(u)}; \qquad C_x^3(h) = \frac{2[1-\cos f_3(u)]}{k_3(u)}.$$

$$C_x^1(h) = C_x^1(\gamma_1); \qquad C_x^2(h) = C_x^2(\gamma_2) = \frac{2}{1+\frac{2}{\pi}ctg\frac{\gamma}{2}\ln tg\left(\frac{\gamma}{2}+\frac{\pi}{4}\right)} \qquad C_x^3(h) = C_x^3(\gamma_3).$$

We've got the general case $C_x(h) = C_x(\gamma)$ including the C. Iacob formula for $C_x^2(h) = C_x(h) = C_x^2(\gamma)$.

Analyzing the values of $C_x(h), C_x(k)$ for the plate, obtained by C. Iacob [2], S. Popp [9], and the tables of $C_x(h)$ for the curvilinear obstacle $C_x h(\gamma)$ [4], in the last situation II3 there is a case where $L=1$ when $\gamma \to \pi$; in this case $\gamma(a^*) = \pi \Rightarrow a^* = 1{,}005; k^* = 6{,}412$ and $h^* = 1/k^* = 0{,}156$. We get the following conclusions regarding the movement behavior and validity conditions for $C_x(h)$ with respect to C_x (unlimited stream), the optimal deflector for maximal resistance [4].

If :

a) $0 < h < h^* \Rightarrow C_x^h = 2h(1-\cos\gamma_3)$;

b) $k \to k^* \cong 6{,}412 \Rightarrow C_x^h \to C_x^{h^*} = 4h^* \cong 0{,}623; \gamma \to \pi \quad (h \to h^*)$;

c) $h > h^*$ and $h \to \infty \Rightarrow C_x(h) \uparrow C_x^3 = \frac{8}{\pi e} \cong 0{,}936$; in this case *h*>0,156*L*.

Table 1

K	2.245	3	4	5	6.142k_0	7
γ	1.571	1.1871	2.251	2.623	3.142	3.359
a^*	1.494	1.219	1.074	1.024	1.005	1.002
C_x	0.891	0.864	0.814	0.747	0.624	0.565

Table 2

K	$\frac{\pi}{6}$	$\frac{\pi}{4}$	$\frac{\pi}{3}$	$\frac{\pi}{2}$	$\frac{2\pi}{3}$	$\frac{3\pi}{4}$	$\frac{5\pi}{6}$	$\frac{11\pi}{12}$	π
γ	0.287	0.623	1.088	2.245	3.584	4.282	4.989	5.700	6.412
a^*	11.747	5.217	2.974	1.494	1.116	1.054	1.024	1.011	1.005
C_x	0.933	0.928	0.919	0.891	0.837	0.797	0.748	0.690	0.624

REFERENCES

[1] V. Barbu, *Metode matematice în optimizarea sistemelor diferenţiale,* Editura Academiei, Bucureşti, 1989;

[2] C. Iacob, *Introduction mathematique a la mechanique des fluids,* Editions Gautier Villars, Paris, 1959;

[3] D. Ionescu, *Introducere în mecanica fluidelor,* Editura Tehnică, Bucureşti, 2004;

[4] M. Lupu and E. Scheiber, *Analytical method for airfoils optimization in the case of nonlinear problems in jet aerodynamics,* In: Mathematical Reports, Romanian Academy, no. 1, p. 33-43, 2001;

[5] M. Lupu and E. Scheiber, *Exact solution for an optimal impermeable parachute problem,* In: Journal of Computational and Applied Mathematics, Elsevier, vol. 147, p. 277-286, 2002;

[6] M. Lupu and F. Isaia, *Utilizarea problemelor la limită inverse la optimizarea operatorilor neliniari în hidroaerodinamică*, In Bulletin of the Transilvania University of Braşov, p. 133-142, 2003;

[7] M. Lupu, Gh. Radu, Şt. Nedelcu and M. Boşcoianu, *New Methods of Optimization Shape for Maximal Drag or Lift Force Airfoils,* Review of the Air Force Academy, The Scientific Informative Review, No. 2(17), pp. 55-62, 2010;

[8] T. Oroveanu, *Mecanica fluidelor vâscoase,* Editura Academiei, Bucureşti, 1967;

[9] S. Popp, *Mathematical models in cavity flow theory,* Editura Tehnică, Bucureşti, 1985.